GEOPOLYMERIC POTENTIAL OF THE ESTONIAN OIL SHALE SOLID RESIDUES: PETROTER SOLID HEAT CARRIER RETORTING ASH

PEETER PAAVER, PÄÄRN PAISTE[*], KALLE KIRSIMÄE

Department of Geology, Institute of Ecology and Earth Sciences, University of Tartu, Ravila 14A, 50411 Tartu, Estonia

Abstract. *In this paper, the geopolymerization of the solid heat carrier (SHC) ash waste produced at Petroter shale oil plants, Viru Keemia Grupp (VKG), Estonia was studied. Different mixtures were prepared to study and evaluate the potential use of this SHC ash for geopolymer-type mortar and cement production and to compare alkali-activated black ash with the material having self-cemented upon hydration with plain water. Mixtures prepared with plain water and NaOH solution show comparable compressive strength development, but the mixture with NaOH affords significantly lower compressive strength values, which can be explained by the absence of an ettringite/monosulphate phase in the NaOH-activated samples. Hydrocalumite precipitated instead of ettringite in the NaOH-activated mixture does not provide the interlocking structure that is found in water mixtures, though the formation of an amorphous geopolymer phase is possibly observed in the NaOH-activated sample after 90 days of curing. Sodium silicate- and Na-silicate/NaOH-activated samples show a strong geopolymerization and development of Ca-Na-Al-silicate gel formed in the pore space of the ash aggregate. However, due to strong shrinkage upon drying, the compressive strength obtained after 7 days of curing is lost in the prolonged curing process, and further research into the causes and prevention of Ca-Na-Al-silicate gel shrinkage is needed.*

Keywords: *alkali activation, oil retorting waste, black ash, geopolymerization, Ca-Na-Al-silicate gel.*

1. Introduction

Geopolymeric binders produced by alkali activation of different solid waste materials as an alternative to common Portland cement constitute an area of rapidly growing interest in building materials research all over the world [1]. This technology applies depolymerization and subsequent repolymerization

---

[*] Corresponding author: e-mail *paarn.paiste@ut.ee*

of crystalline and/or amorphous aluminosilicate structures under alkaline treatment, resulting in hardened materials that can provide performance comparable to traditional cementitious binders for a range of applications. In addition to the beneficial reuse of solid waste from energetics, ore processing and/or the chemical industry, it is also of utmost importance that this approach allows significant reduction in the carbon footprint and energy consumption in the production of the construction materials [1].

The Estonian energy sector employs oil shale-type fossil fuel, a widespread sedimentary rock containing kerogenous organic matter that can be pyrolysed to extract shale oil or burnt for heat and power generation [2]. Total world resources of shale oil are conservatively estimated at 4.8 trillion barrels, but production of shale oil is, compared to petroleum, more expensive due to the relatively high mining, processing and environmental costs. Nevertheless, oil shale is processed in several countries worldwide. The Estonian oil shale industry is the largest in the world with the annual mining output in the past five years of approximately 14–17 Mt, currently providing about 77% of the energy generated in Estonia [3]. The majority (approx. 80%) of mined oil shale is utilized at thermal power plants (TPPs) for electricity and heat generation, while most of the remaining oil shale (19%) is used for retorting shale oil and shale gas [2]. It is foreseen that the share of shale oil production in oil shale usage in Estonia will increase in the coming decades [4].

Retorting of shale oil and gas is performed either by using gas as the heat carrier or by the solid heat carrier (SHC) process, which is the most commonly employed pertinent technology [5, 6]. Currently, there are two major SHC technology modifications used for shale oil production in Estonia – Petroter technology used at Viru Keemia Grupp (VKG) and Enefit employed at Eesti Energia. The mineral matter content of oil shale can be as high as 80–90 wt%, but in the mined shale beds it is approximately 40–50 wt% [7]. Due to the high mineral matter content, about half of the processed oil shale is left as a solid waste. At the current processing rates, each year, 6–8 Mt of oil shale solid waste is produced. The ash formed at TPPs accounts for the majority of this oil shale solid waste, while approximately 1.5 Mt of shale oil retorting waste is produced annually [5]. The secondary beneficial use of oil shale processing waste is limited (< 5% of total), and only the ash from thermal power plants is used. Solid residues from shale oil retorting are currently not used and become landfilled [5, 8].

The motivation for this study was to find new ways and methods for beneficial use of oil shale waste, specifically as a low-cost building material. The aim of this contribution is to study and evaluate the potential application of kukersite oil shale SHC retorting waste remaining at Petroter shale oil plants for geopolymer-type cement and mortar production. Emphasis is placed on a comparison of compression strength development in the alkali-activated waste with the self-cementation of the material obtained upon hydration with plain water. Hydrothermal alkaline (NaOH and KOH) treatment of oil shale combustion ash at high temperatures can produce Al-

substituted tobermorite [9, 10] which is a typical constituent of ordinary cement based concrete [11], but to our knowledge, the geopolymeric potential of SHC retorting waste for construction applications and its alkaline activation under ambient conditions have not been studied before.

2. Material and methods

The solid heat carrier ash studied was sampled at the Petroter-type SHC retort and was provided by VKG. The Petroter SHC process results in dark grey retorting ash (also known as "black ash") that contains up to a few percent of organics [12, 13]. During retorting, oil shale is heated in the absence of oxygen to the temperature (approx. 400 ℃) at which its organic part – kerogen – is decomposed and pyrolysed into gas, condensable oil and solid residue, while the inorganic mineral matrix is retained in the form of spent shale. During the SHC process, the retorting residue is heated/burnt up in the presence of oxygen and directed back to the retort chamber as the heat carrier [2].

The physical, chemical and mineralogical properties of Petroter SCH retorting ash (black ash) were studied earlier by Talviste et al. [13]. This study shows that black ash contains several reactive phases (e.g., lime, belite) that can react with water, and therefore, the hydrated black ash sediment potentially has cementitious properties. Black ash contains a notably low amount (< 5%) of lime (CaO), suggesting that carbonation reactions do not contribute much to the stabilization of the sediment. However, black ash contains a considerable amount of cement clinker minerals (belite and ferrite), which, upon hydration, form a C-S-H gel-like mass providing cementation of the material. Hydration of ferrite (C4AF) occurs fairly quickly, but the contribution of the hydrated ferrite to the strength is rather subdued (6–8 MPa in the pure compound). Belite hydration in cement pastes occurs over 60–90 days, but its final strength peaks at approximately 40 MPa for the pure compound [14]. Moreover, upon long-term hydration, black ash develops another binding phase – hydrocalumite. As a result, black ash mortars show uniaxial compressive strength values > 6 MPa after 90 days of curing under ambient air conditions [13].

Cementation of black ash was studied in four series of monolithic samples prepared by mixing the dry black ash with the following activators: water, sodium silicate (Na-silicate), 5 M sodium hydroxide solution and sodium silicate + sodium hydroxide (Table 1). The amount of water used in the mixtures was equal to the maximum water content in fresh ash under pore space saturation conditions determined experimentally prior to mixing. Cylindrical specimens of black ash/activator mixtures were prepared and stored in PVC tubes under ambient conditions. For each mixture, three parallel specimens were made and tested. All sodium silicate-based activator solutions were prepared so that the Na_2O content in the additive was 10% (w/w), to normalize the alkaline component in the mixtures.

Table 1. Composition of mixtures used in experiment

Mixture	Water/ash ratio, wt%	Na_2O/ash, wt%	SiO_2/Na_2O molar ratio
Ash-H_2O	0.5		
Ash-NaOH	0.5	0.09	
Ash-NaOH + SS	0.5	0.1	2.72
Ash-SS	0.5	0.1	1.5

Note: SiO_2/Na_2O and Na_2O values apply to the alkali activator components and not the overall composition of the mixtures. SS – Na-silicate.

The self-cementing properties of black ash were evaluated by uniaxial compressive strength tests under continuous loading (20 kPa·s^{-1}) until the specimen broke. Compressive strength was measured in three replicates after 7, 28 and 90 days. For testing, cylindrical specimens were removed from the PVC tubes. Altogether, 36 compressive strength tests were conducted in the Laboratory of Sedimentology at the Department of Geology, University of Tartu.

The mineral and chemical compositions of the fresh black ash and solidified samples were examined using X-ray diffraction (XRD) on a Bruker D8 Advance diffractometer employing Cu$K\alpha$ radiation and X-ray fluorescence (XRF) analysis on a Rigaku Primus II spectrometer, respectively. The mineral composition of the hardening material was analysed in the specimens used in compressive strength tests, i.e. after 7, 28 and 90 days. The chemical composition of the initial fresh ash and of samples after 90 days of curing was determined. For XRD and XRF analyses, the materials were dried at 105 °C for 2 hours and ground in a planetary ball mill. The quantitative mineral composition of the unoriented powdered samples was modelled using the Rietveld method in Bruker Topas 4.0 code. To determine the quantity of the amorphous glassy phase that is not detected by the conventional XRD method, the test specimens were spiked with 10 wt% of ZnO prior to XRD measurement. The amorphous phase absorbs X-rays and causes an apparent lower ZnO content than was spiked in the sample. The amorphous phase content was calculated from the difference between the added and measured spike phases assuming the aluminosilicate composition of the glass. Total organic carbon in the original fresh black ash was measured as the loss on ignition at 550 °C for 2 hours, and the total loss on ignition of all samples was measured at 950 °C for 2 hours.

Scanning electron microscopy (SEM) imaging of test samples was performed on a Zeiss EVO MA15 SEM equipped with an Oxford AZTEC energy dispersive X-ray analytical system. The samples were analysed both uncoated in the variable pressure mode and coated with gold or platinum in the high vacuum mode.

3. Results and discussion

3.1. Mineral and chemical composition

3.1.1. Fresh black ash

The average mineral composition of the crystalline phases and an amorphous phase of the fresh black ash (Fig. 1, Table 2) is dominated by calcite (26.8 wt%), quartz (11.7 wt%) and K-feldspars (14.3 wt%). The content of dolomite is on average 8.5 wt%. All of these components are also characteristic of raw oil shale. In addition, black ash contains secondary phases formed during thermal treatment of oil shale: authigenic calcium silicates (14 wt%), periclase (7.5 wt%), free lime (2.1 wt%) and oldhamite (3.6 wt%).
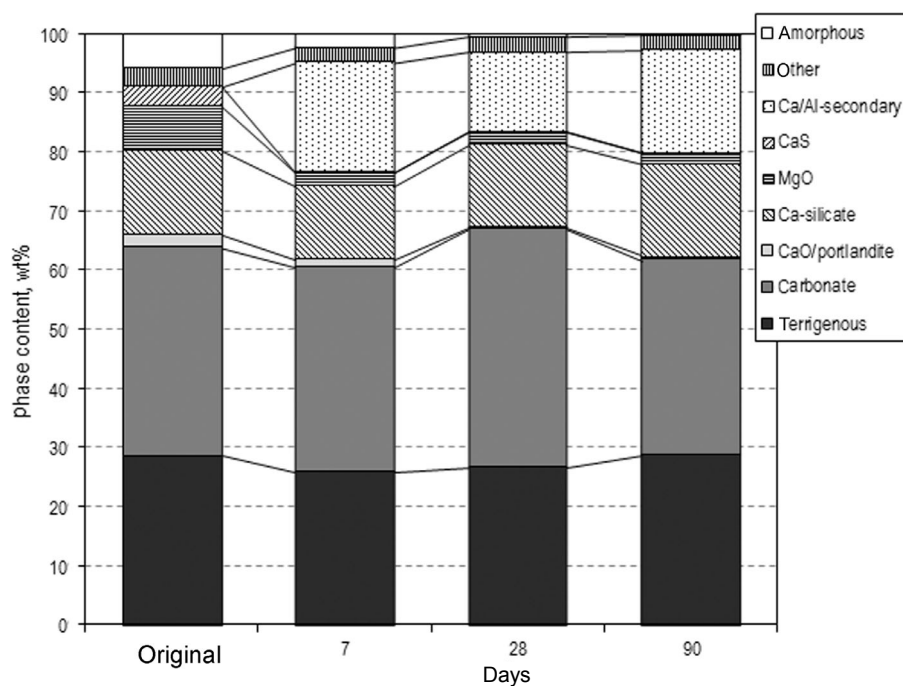

Fig. 1. Mineral composition of fresh black ash (original) and water-mixed samples after 7, 28 and 90 days of curing. Legend: Amorphous = aluminosilicate composition, amorphous glass phase; Other = magnetite, hematite, gypsum and anhydrite; Ca/Al-secondary = sum of ettringite and hydrocalumite; Ca-silicate = sum of C_2S, merwinite and wollastonite; CaO/portlandite = sum of lime and portlandite; Carbonates = sum of calcite, vaterite and dolomite; Terrigenous = sum of quartz, K-feldspars and mica/muscovite.

Table 2. Mineral composition, wt%

Sample Phase/days	Fresh black ash	Fresh black ash + water			Fresh black ash + NaOH			Fresh black ash + Na-silicate/NaOH			Fresh black ash + Na-silicate		
	Original	7	28	90	7	28	90	7	28	90	7	28	90
Quartz	11.7	11.7	11.9	10.7	10.1	13.3	8.4	8.7	10.6	7.7	7.4	6.7	7.8
Orthoclase	14.3	12.5	11.3	12.3	12.0	11.5	10.0	11.2	10.9	10.5	11.8	10.4	12.1
Muscovite/mica	2.6	1.7	3.4	5.7		1.5	5.1	5.9	6.6	7.1	6.9	7.1	7.2
Calcite	26.8	23.2	28.4	25.6	23.6	25.8	21.7	19.6	21.6	21.0	18.9	16.5	19.2
Vaterite		2.9	tr	1.5	2.4	2.7	2.9	1.4	1.3	1.5	1.5	1.9	2.1
Dolomite	8.5	8.6	11.8	6.0	6.6	7.1	4.7	5.7	3.9	5.9	5.7	5.5	5.0
Lime	2.1												
Portlandite		1.2	tr	tr	1.5	2.1	0.7						
Periclase	7.5	2.2	1.9	1.9	2.5	2.7	2.1	3.8	3.3	2.5	3.2	2.1	2.1
C$_2$S	3.2	5.7	6.7	7.1	5.8	6.9	6.8	2.7	2.2	2.3	2.3	2.4	2.5
Merwinite	5.2	2.2	1.6	1.3	2.8	2.8	2.4	2.6	2.9	2.1	2.0	2.3	1.5
Melilite	4.2	2.0	2.6	2.9	3.8	3.0	2.1	2.8	2.3	3.0	2.6	3.3	2.6
Wollastonite	1.5	2.5	3.1	4.3	3.8	3.4	3.1	4.0	4.7	4.9	3.7	4.3	4.2
Oldhamite	3.6				0.7	0.6	tr	2.0	1.0	0.7	1.7	0.8	0.8
Anhydrite	1.1												
Gypsum		0.9	0.7	1.0	1.0	1.3	2.3						
Hydrocalumite		13.9	6.0	11.1	17.9	13.3	16.5						
Ettringite		4.7	7.6	6.3									
Smectite					0.5	0.8	2.1						
Hematite	1.1	0.5	tr	0.6	tr	tr	tr	0.8	0.8	0.6	0.7	tr	0.8
Magnetite	0.9	1.3	1.8	1.2	1.1	1.6	1.2	0.9	1.0	0.9	0.7	0.9	0.6
Amorphous phase	5.7	2.2	tr	tr	3.7	tr	7.1	28.2	27.0	29.1	31.0	35.4	31.5

Note: tr – trace amount (< 0.5%).

Oldhamite is a CaS phase that is particularly characteristic of black ash and does not occur in thermal power plant (TPP) ashes that are a byproduct of oil shale thermal combustion. Oldhamite forms under oxygen deficiency conditions in the reaction between CaO and H_2S. Another mineral indicating oxygen deficiency during black ash formation is the partly oxidized Fe-oxide mineral magnetite (Fe_3O_4 ($FeO \cdot Fe_2O_3$)), while in the TPP ashes, hematite Fe_2O_3 is typically present. In addition, a dehydrated mica-like clay phase was identified in black ash. The content of the amorphous glass phase in the fresh black ash varies from 3.0 to 7.2 wt%, and the average content of the amorphous phase is 5.7 wt%.

The chemical composition of fresh ash (Table 3) corresponds to the mineral composition of the samples studied and is dominated by CaO and SiO_2 that account on average for 32 and 21 wt%, respectively. The content of MgO, Al_2O_3 and Fe_2O_3 in fresh ash is on average 8.2, 5.3 and 3.7 wt%, respectively, and the sulphur content averages 2.0 wt%. The carbon content (C_{total}) is approximately 7.0 wt%, and that of organic carbon (C_{org}) is 1.5–2.2 wt%.

Table 3. Chemical composition of the fresh black ash and mixtures after 90 days of curing, wt% (average of three samples)

Sample Compound	Fresh black ash	Fresh black ash + water	Fresh black ash + NaOH	Fresh black ash + Na-silicate/ NaOH	Fresh black ash + Na-silicate
SiO_2	21.23	18.88	24.67	32.47	38.12
Al_2O_3	5.27	4.56	4.47	3.57	3.24
TiO_2	0.16	0.25	0.32	0.24	0.24
Fe_2O_3	3.65	3.02	3.47	2.97	2.62
MnO	0.07	0.06	0.06	0.05	0.05
CaO	31.89	29.72	28.26	25.24	22.15
MgO	8.15	11.01	5.84	6.23	5.61
Na_2O	0.11	0.24	2.97	3.53	3.43
K_2O	2.58	2.38	1.92	1.73	1.56
Cl	0.34	0.67	0.27	0.23	0.21
P_2O_5	0.11	0.19	0.08	0.07	0.06
S_{total}	1.97	3.42	1.11	0.88	0.77
LOI 950 °C	21.33	25.54	26.47	22.74	21.89
C_{org}	1.86	n.d.	n.d.	n.d.	n.d.

Note: LOI – loss on ignition (950 °C), n.d. – not determined.

3.1.2. Black ash-water system

The mineral and chemical compositions of black ash and water mixtures are different from the composition of the fresh black ash because of the hydration reactions (Fig. 1, Tables 2 and 3). The mineral composition of water-treated black ash samples after 7 days of hydration is principally similar to that of the original black ash. The content of carbonate mineral phases (calcite and dolomite) is approximately 35 wt%. The content of terrigenous mineral phases (quartz, orthoclase and mica-muscovite) is approximately

26 wt%, and the content of the secondary calcium silicate (Ca-silicate) phases is approximately 12.5 wt%, whereas that of periclase (MgO) is 2.2% (Fig. 1). The major difference in mineral composition between the hydrated samples after 7 days and fresh ash is the disappearance of oldhamite (CaS) and the formation of the secondary Ca-Al hydrate phase hydrocalumite and the Ca-Al sulphate-hydrate phase ettringite. In fresh ash, the oldhamite content is on average 3.6 wt%, but after 7 days of hydration, practically all of the oldhamite has been dissolved. CaO has also disappeared after 7 days of hydration, and as a result, calcium hydroxide (portlandite [$Ca(OH)_2$]) is formed. The content of hydrocalumite and ettringite after 7 days is, respectively, 13.9 and 4.7%. There is also a change in the amorphous phase content, which in fresh ash is approximately 5 wt% and in the 7-day sample, 2 wt%. However, the relative error in amorphous phase measurements can be as high as 30 to 50%, and this change can be just an analytical variation. After 28 and 90 days, the changes in the mineral composition of the water-hydrated samples compared to that of the mixture after 7 days are rather small. Only portlandite has practically disappeared, and the relative content of calcite shows an increase, which is evidently due to portlandite carbonation. There is also a slight increase in the ettringite content, up to 7.6 wt%, and the amorphous phase is practically absent, as its content is less than 1 wt% after 28 and 90 days.

The chemical composition of all materials studied was measured in the original fresh ash and after 90 days of curing. In the mixture with water, the dominant elements were magnesium, calcium and silicon, referred to as the respective oxides (Table 3). During the curing period, there were only slight changes in the chemical composition of water mixtures. There is an increase in Loss on Ignition (LOI) performed at 950 °C in the black ash-water mixtures that is evidently due to carbonation of portlandite and capture of atmospheric CO_2 for additional calcite precipitation. This added CO_2 is released during LOI determination due to calcite decomposition at temperatures > 800 °C.

3.1.3. Black ash-NaOH system

Evolution of the mineral composition in samples treated with NaOH activator is similar to the changes in the samples mixed with plain water (Fig. 2). The content of the dominant secondary phases formed in samples treated with NaOH differs from that in water-treated samples (typically ± 5 wt%). However, there are a few specific differences between the water-mixed and NaOH-activated samples. Compared to the samples treated with water the most important difference is the absence of ettringite in the NaOH-activated mixture. Additionally, the content of hydrocalumite is approximately 4 wt% higher in the 7-day samples and 5 to 7 wt% higher in the 28- and 90-day samples than in specimens mixed with water. Moreover, the authigenic clay mineral identified as smectite (montmorillonite) appears
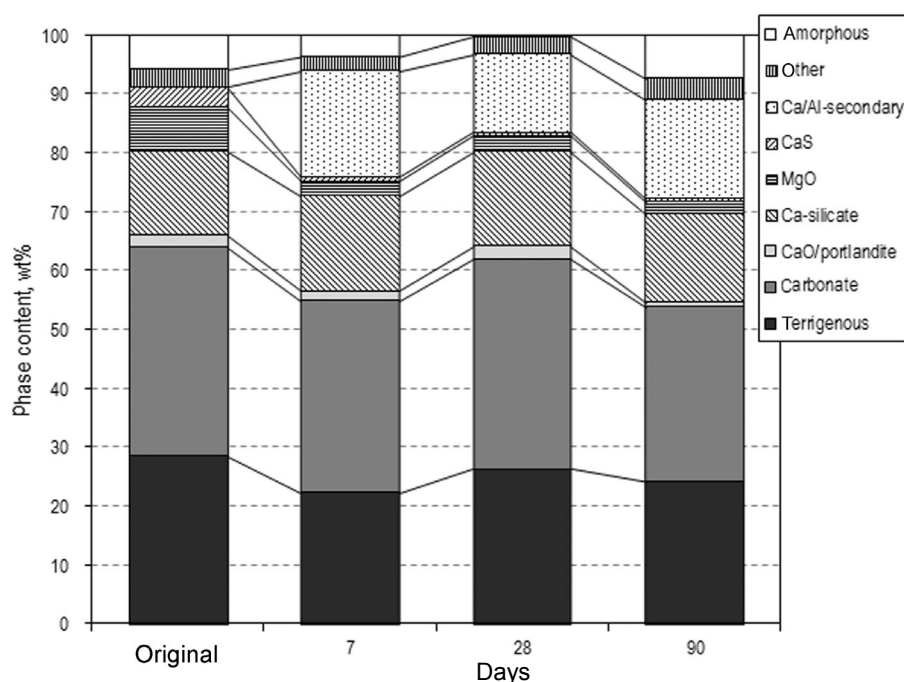
Fig. 2. Mineral composition of fresh black ash (original) and NaOH-activated samples after 7, 28 and 90 days of curing. For the legend, see Figure 1.

in low content (0.5 wt%) after 7 days of hydration and has a slightly higher content (2.1 wt%) after 90 days (Table 2).

There is also an increase in the amorphous phase content after 90 days, which could indicate the formation of an amorphous geopolymer phase, but as mentioned earlier, the determination of the amorphous phase is not very accurate and must be considered with caution. However, the formation of uthigenic smectite clay in this mixture indicates dissolution and recrystallization of Si and Al phases, which supports the observed increase in the amorphous phase (Fig. 2).

The major change in the chemical composition of fresh ash and the NaOH-water mixture after 90 days of curing (Table 2) is the increase in Na_2O content, which is due to the addition of NaOH. Similarly to the ash-water mixtures, there is also an increase in LOI values due to the carbonation of portlandite.

3.1.4. Black ash-sodium silicate and sodium silicate/NaOH system

The mineral composition of the black ash specimens mixed with sodium silicate-based solutions differs considerably from that of the samples treated with water or NaOH. A distinct and major change compared to the fresh black ash samples and water- and NaOH-mixed samples takes place in the content of the amorphous phase, which has risen from the 5.7 wt% in fresh

ash to approximately 30 wt% in 7 days and to 35 and 31 wt% in 28 and 90 days, respectively (Figs. 3 and 4). This change is due to the formation of amorphous Ca-Na-Al-silicate gel from the reaction between the Na-silicate solution and the minerals present in black ash. As a result of the amorphous phase addition, there is a decrease in the relative content of the carbonate phases (calcite, vaterite and dolomite) from 35 wt% of the fresh ash composition to approximately 26 wt% in 7 days and also a relative decrease in the periclase and oldhamite phases from 7.5 wt% and 3.6 wt% to approximately 2 wt% and less than 1 wt%, respectively, over the curing period. The free CaO (lime) has totally disappeared after the hydration, as was also observed in mixtures with water.

There are no significant mineralogical differences between the samples activated by Na-silicate and those treated with Na-silicate + NaOH-diluted solutions. Differences in mineral composition between these two different mixtures vary a few percent (Figs. 3 and 4, Table 2), indicating similar changes in both mixtures. The observed changes in the chemical composition of Na-silicate and Na-silicate/NaOH mixtures compared with the original fresh ash are related to the addition of Na and Si. In the samples mixed with Na-silicate, the SiO_2 content has increased to 32.5 wt% in the sample prepared with Na-silicate + NaOH and to 38 wt% in the sample prepared with only Na-silicate.
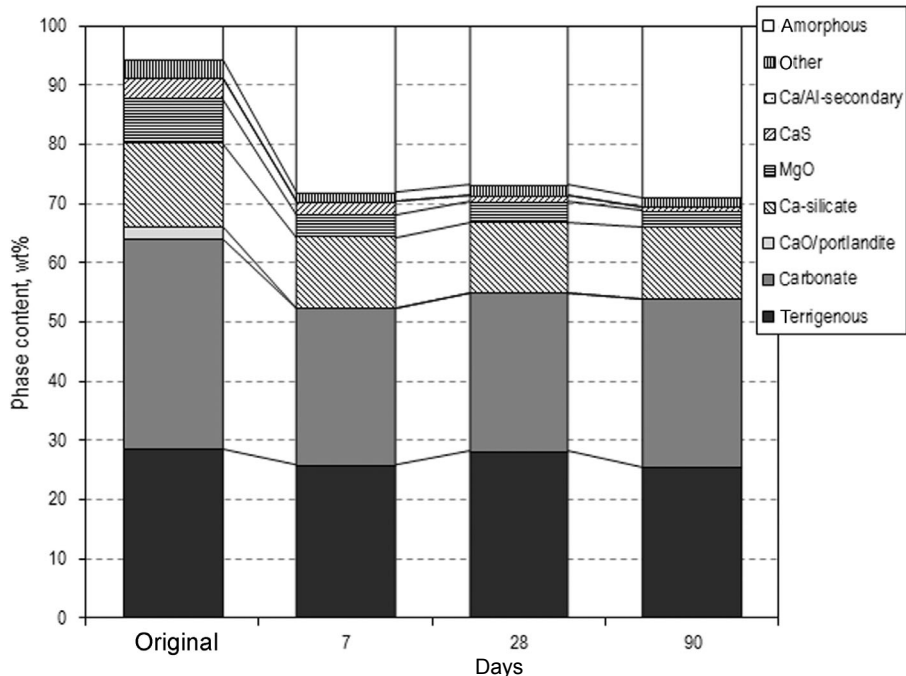

Fig. 3. Mineral composition of fresh black ash (original) and sodium silicate-activated samples. For the legend, see Figure 1.
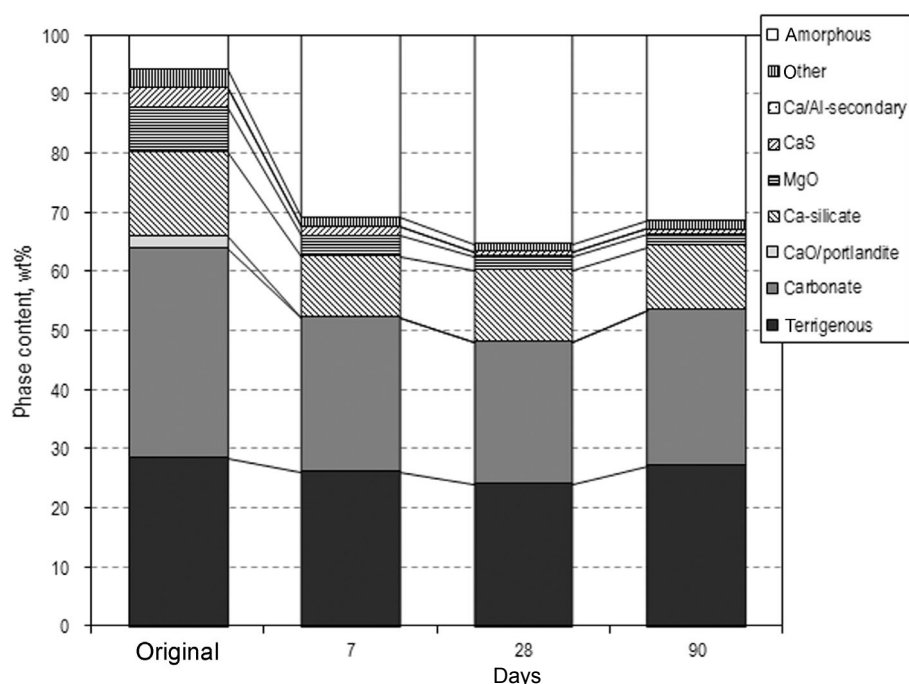
Fig. 4. Mineral composition of fresh black ash and Na-silicate/NaOH-activated samples after 7, 28 and 90 days of curing. For the legend, see Figure 1.

3.2. Microstructure

Scanning electron microscopy (SEM) analysis of the original black ash shows that the material is fine-grained with a particle size generally less than 60 μm, while particles with a diameter < 20 μm dominate (Fig. 5a). The particles are irregular in shape, and the finest particles are somewhat aggregated into lumps approximately 20–30 μm in size (Fig. 5b). Samples mixed with water (Figs. 5c–d) show intensive cementation and development of secondary Ca-Al and Ca-Al-sulphate minerals in the material pore space. The ash particles are covered by secondary precipitates, and bonds between the particles are generated by interlocking needle- and lath-shape authigenic minerals that can be identified by crystallite morphology and chemical composition as hydrocalumite and ettringite. Secondary calcite precipitation can also be observed (Fig. 5d). When comparing samples after 7 and 90 days of curing, a significant increase in the density of the secondary mineral crystallites may be noted (Figs. 5c–d).

Mixtures activated with only NaOH solution show a microstructure similar to that of water-mixed samples, but ettringite is not identified and the pore space is filled with hydrocalumite platy crystals and crystal aggregates (Figs. 5e–f). This finding agrees well with the mineralogical analysis showing the absence of ettringite and the presence of abundant hydrocalumite in
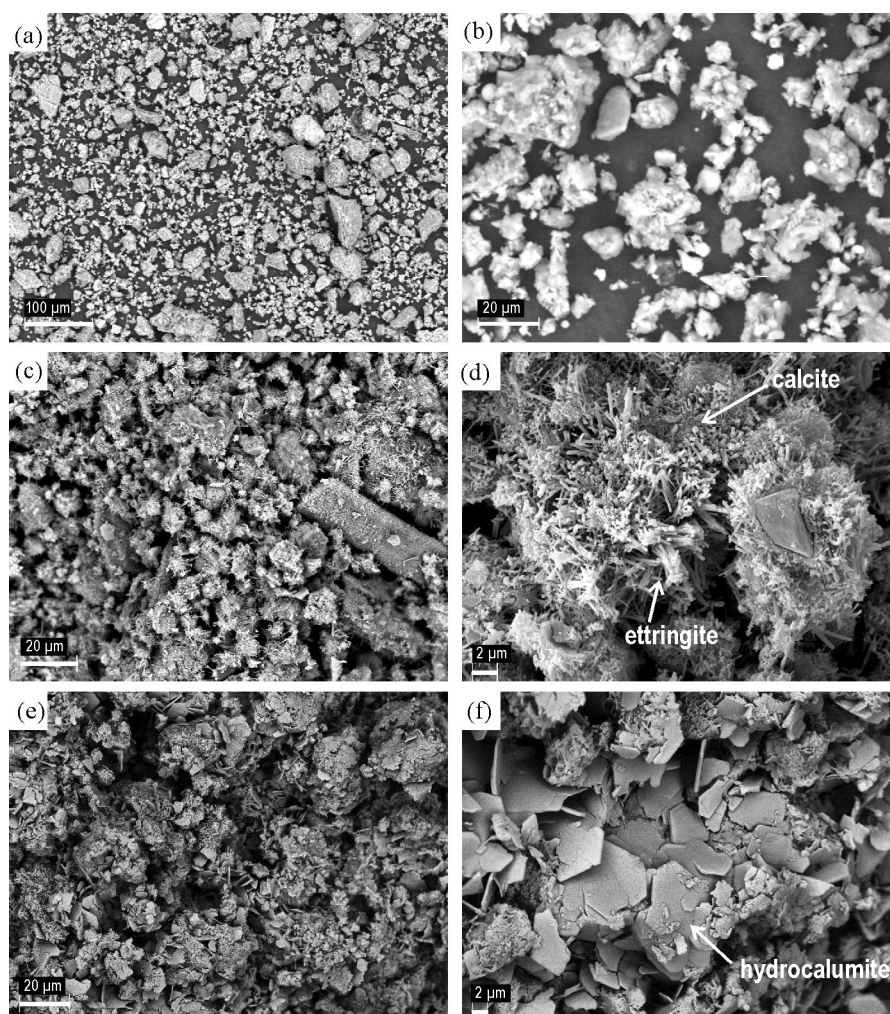
Fig. 5. SEM images: (a), (b) fresh black ash; (c) ash-water mixtures after 7 days of curing; (d) ash-water mixtures after 90 days of curing; (e), (f) black ash and NaOH mixture after 90 days of curing. Images are taken in the variable pressure mode with a backscattered electron detector.

the ash-NaOH system. The size of the hydrocalumite crystallites is generally 2–5 μm, but in places, larger crystals exceeding 10 μm in size can be observed (Fig. 5f).

The microstructure of Na-silicate/NaOH and Na-silicate-activated mixtures is considerably different from that of the water and NaOH mixtures and is similar to each other (Figs. 6a–d). SEM images of silicate containing activator solutions show that the solidified material is filled in by amorphous glassy-like masses, which agrees with the significant increase in the amorphous phase revealed in the XRD analysis of these mixtures. Under
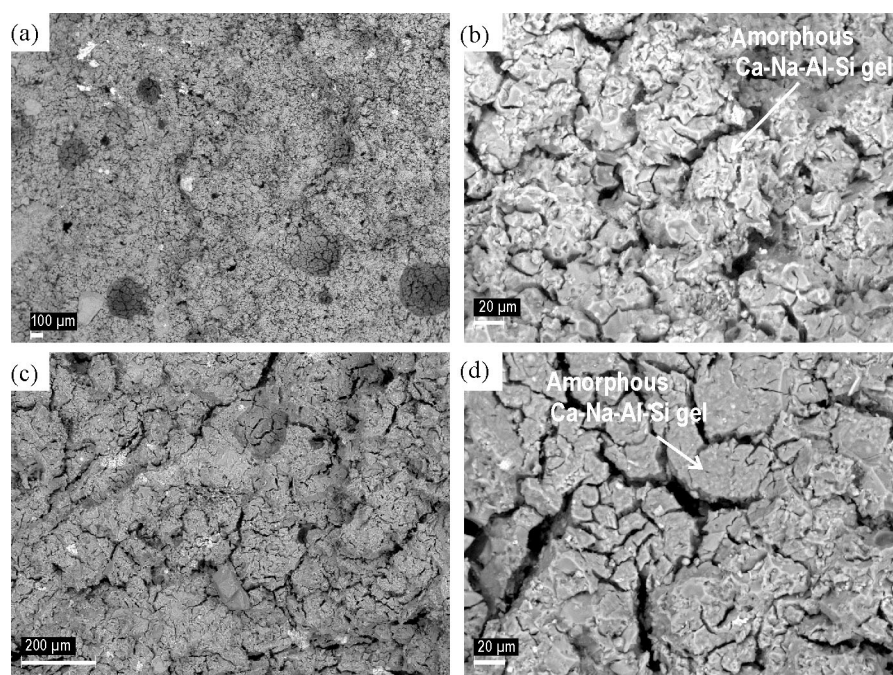
Fig. 6. SEM images: (a), (b) black ash and Na-silicate solution mixture; (c), (d) black ash and Na-silicate + NaOH mixture after 90 days of curing. Images are taken in the variable pressure mode with a backscattered electron detector.

SEM, the energy dispersive analysis of the material shows that it is composed of a Ca-Na-Al-silicate gel-like matrix, filling the area between the unreacted ash particles. Ca-Na-Al-silicate gel (geopolymerized "glass") is strongly fractured and practically all surfaces are cut with dense fracture networks. Fracturing already occurs in samples after 7 days of curing but is specifically intense in samples analysed after 90 days. However, the development of cracks can also be due to the dewatering of the gel under vacuum conditions in the electron microscope, but the same pattern was observed both under high and low vacuum conditions, indicating that the fracturing is not induced solely by the vacuum but also by the recrystallization and dewatering of the geopolymerized gel during the curing.

3.3. Uniaxial compressive strength

The uniaxial compressive strength was measured in three replicates in all four different mixtures after 7, 28 and 90 days. After 7 days of curing, black ash mixed with the sodium silicate-diluted solution afforded good results regarding compressive strength, which exceeded 8 MPa on average and peaked at > 10 MPa (Fig. 7a). However, after 28 days of curing, the compressive strength dropped below 5 MPa. Though after 90 days of curing the compressive strength values had increased slightly, they still remained low
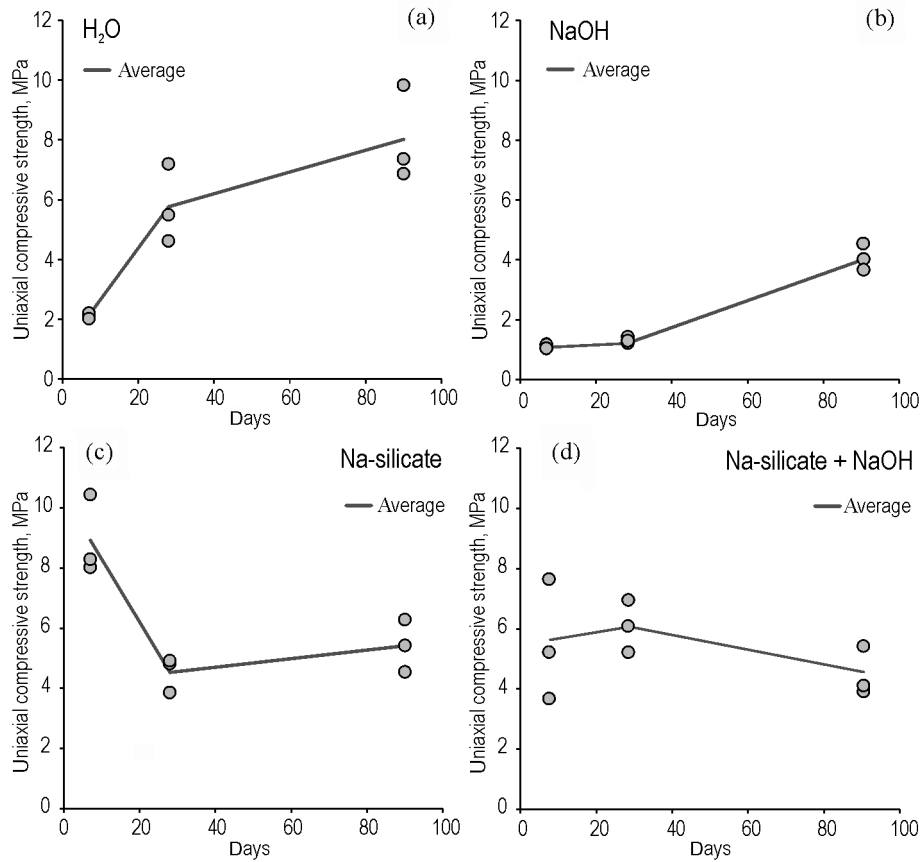
Fig. 7. Uniaxial compressive strength values of tested mixtures after 7, 28 and 90 days of curing: (a) black ash-water mixtures; (b) NaOH-treated mixtures; (c) sodium silicate-treated mixtures; (d) Na-silicate + NaOH-treated mixtures.

compared to the figure this mixture afforded initially. This drop in compressive strength in sodium silicate-treated samples was accompanied by a significant reduction in sample sizes (measured as the diameter and length of the tested cylinders) already after 7 days of curing, and the diameter and length of the samples decreased up to 10% after 90 days of curing. The mixture of black ash and Na-silicate diluted with NaOH also afforded rather high compressive strength values after 7 days of curing, which varied from 3.6 to 7.6 MPa. However, after 28 days, this value was subdued to 6 MPa on average. After 90 days of curing, the uniaxial compressive strength dropped below 5 MPa (Fig. 7b), whereas the dimensions of the test cylinders were decreased on average 5% after 90 days of curing, similarly to the sodium silicate-treated samples.

Unlike the samples treated with Na-silicate and the Na-silicate + NaOH diluted solution, those mixed with only NaOH maintained the growth in

uniaxial compressive strength over 90 days of the curing period from, on average, 1.2 and 1.4 MPa after 7 and 28 days of curing, respectively, to 4.2 MPa after 90 days (Fig. 7c). This growth would indicate that some geopolymer-like bonds were developed after 90 days of curing, which agrees with the increase in the amorphous phase content in these samples after 90 days, as revealed in XRD analyses (Fig. 2). However, the final compressive strength of these mixtures remained much lower than the initial strength obtained in the Na-silicate mixtures and even lower than what was observed in the Na-silicate (+ NaOH) mixtures after 90 days of curing (Figs. 7a–b).

Samples that were prepared as black ash and water mixtures also maintained a slow but steady increase of compressive strength over the curing period, but unlike the samples treated with NaOH, the strength achieved after 90 days was comparable to the compressive strength obtained after 7 days in Na-silicate and Na-silicate + NaOH activated samples (Fig. 7d). After 7 days, samples mixed with water exhibited a compressive strength of only 2 MPa, but after 28 days, the average strength of the samples was already close to 6 MPa, and after 90 days, approximately 8 MPa, with the strongest tested specimen peaking at nearly 10 MPa (Fig. 7d).

3.4. Hydration, geopolymerization and the development of compressive strength

The fresh black ash contains several reactive phases that are capable of reacting with water and/or NaOH, and Na-silicate to form cementitious bonds in the material. However, development of the cementation and build-up of the compressive strength are principally different in mixtures made with plain water and in activated materials. In mixing with plain water, several hydration reactions occur. First, the free CaO (lime) reacts quickly with water, forming portlandite. Under open conditions where the atmospheric CO_2 can enter the material, portlandite reacts and secondary calcium carbonate is precipitated as indicated in the mineralogical changes as well as observed in the SEM of the black ash-water mixtures. In the water-mixed samples, the secondary Ca-Al-sulphate phase (ettringite) and the Ca-Al-phase (hydrocalumite) also started to precipitate. Formation of ettringite and hydrocalumite is a characteristic process in the hydrated oil shale ash and semicoke deposits [5, 8, 15–17]. Sulphate needed for ettringite formation was possibly delivered by the CaS dissolution that disappeared quickly after the beginning of our experiments. However, it is particularly interesting that an earlier study of black ash hydration [13] did not observe significant ettringite formation. In our experiments, the content of ettringite measured in water-treated samples was not very high (max 7.6%) either, especially compared with the hydrated oil shale ash from TTPs and the semicoke waste from the shale oil retorting processes where ettringite can form up to 30 wt% of the crystalline phases [5]. However, ettringite plays an important role in the self-cementation of semicoke and power plant deposits by forming interlocking meshes of needle-like crystals filling the pore space, which is

evident from the SEM analysis. Additionally, Talviste et al. [13] have suggested that possibly a metastable amorphous monosulphate or Ca-monosulphate-aluminate hydrate phase had precipitated together with ettringite [18]. This phase is not detectable by the XRD method but is morphologically similar to ettringite and can transform into stable ettringite upon dehydration/recrystallization and thus contribute to the development of compressive strength in the hydrated black ash. Both the secondary Ca carbonate precipitation and ettringite formation require access to atmospheric CO_2 and some time. Liira et al. [19] have noticed that in TPP ashes, ettringite does not form before 7 days of hydration, and its formation continues for up to 30 days, whereas ettringite is a stable phase only at elevated pH levels (pH 9–13) and is slowly dissolved by percolating unsaturated precipitation water and becomes replaced by calcite and Ca-sulphate hemihydrate phases, meaning that ettringite-based cementation developed in ash-water reactions is not stable in an open atmospheric environment over the long term.

The mineral composition as well as the development of compressive strength in the samples activated with NaOH dilution is at first rather similar to those of the samples mixed with water, and although the final compressive strength is lower, it is achieved more slowly, and there is no ettringite observed in the XRD or SEM analysis of this mixture. Possibly, the lower compressive strength values of the NaOH-activated samples specifically in the first and final stages of the experiment compared with those of the water mixtures in the same stages are due to the absence of needle-like ettringite and/or Ca-monosulphate crystallites that in the ash-water mixtures form a rigid connection between the ash particles. At high NaOH molar concentrations when pH 14 is maintained, the ettringite formation depends on the activity of calcium in the solution, whereas the formation of calcium hydroxide and the sodium-substituted monosulphate phase competes with the ettringite formation [20]. In black ash systems, it is evident that due to abundant reactive Ca phases, the activity of Ca is high, and in the presence of NaOH, the ettringite precipitation is suppressed. Instead, hydrocalumite is the dominant cementitious secondary phase despite its platy crystalline structure; however, it does not provide the similar interlocking and overall compressive strength as the ettringite meshes. Nevertheless, it is possible that the increase in strength by 90 days of curing is due to the formation of an amorphous geopolymer phase indicated by the increase in the amorphous phase content in the XRD analysis, but at the present state of knowledge, it is not fully clear what is the mechanism behind it and whether the geopolymerization occurs in the NaOH-activated samples.

Geopolymerization with formation of the amorphous Ca-Al-Si matrix and development of initially high compressive strengths is evident in Na-silicate and Na-silicate/NaOH-activated samples. However, the behaviour of these samples is remarkably different from that of the black ash and water mixture and also the NaOH-activated samples. Both of the sodium silicate-containing

mixtures already show high strength values after 7 days of curing, amounting to 10.4 MPa in the sodium silicate-activated ash and to 7.75 MPa in Na-silicate/NaOH-activated samples. However, in the latter case, the values did not change much with extended curing time, and in the former case, the values dropped significantly after curing for 28 days with slight improvement after 90 days. The initial good compressive strength of these mixtures is evidently provided by Ca-Na-Al-silicate gel formation in the pore space of the ash aggregate. However, the considerable decrease of the compressive strength or inhibition of its development in test samples made using Na-silicate and Na-silicate/NaOH as activators upon prolonged curing is evidently related to the strong dry-shrinkage of the geopolymer pastes, which is exemplified by the dense microfracturing and development of cracks penetrating the cured samples. The shrinkage of the sodium silicate-activated pastes was approximately 10% of the initial diameter of the test samples, whereas the shrinkage of the test samples prepared from mixtures with the Na-silicate/NaOH activator was less but still 5% of the original dimensions after curing under ambient conditions. The dry-shrinkage occurred within the first week of curing and no subsequent shrinkage over the prolonged curing period was observed.

Shrinkage with a decrease in volume is a very common phenomenon in ordinary concrete [21] and also in geopolymers [22]. Gilbert [21] distinguished several types of shrinkage: plastic shrinkage, chemical shrinkage, thermal shrinkage and drying shrinkage, the last typically accounting for the largest proportion of the total long-term shrinkage in concrete and geopolymers. Factors that affect the drying of mortars also affect the magnitude and rate of development of drying shrinkage, including the type and content of cement or geopolymer binder/activator, water content and water-to-cement ratio, type of aggregate, maximum size and its proportion in the concrete, relative humidity and the size and shape of the member [23]. In geopolymers, the shrinkage is primarily affected by curing temperature and liquid-to-ash ratio, whereas a stronger geopolymer with a smaller shrinkage can be produced at high curing temperature while the shrinkage increases significantly with the increase in liquid-to-ash ratio from 0.4 to 0.7 [24]. More importantly, Ridtirud et al. [24] concluded that the effect of NaOH concentration on compressive strength is small but quite significant on shrinkage. A high NaOH concentration (12.5 M) produces a geopolymer with high shrinkage compared to that achieved with a low NaOH concentration (7.5 M), and also the geopolymer with a high sodium silicate-to-NaOH ratio of 3.0 gives low drying shrinkage compared to other geopolymers with the sodium silicate-to-NaOH ratios of 0.3–1.5. In our study, the samples were cured under ambient conditions in the laboratory environment, and therefore, the drying of the Ca-Na-Al-silicate gel matrix was slow and possibly led to a significant loss in volume and the development of drying cracks. Although the liquid-to-ash ratio in the test samples was approximately 0.5, which is within the acceptable range, we would conclude

that it still led to the shrinkage and significantly reduced compressive strength. Further studies are needed to test the effect of curing temperature and solid/water ratio on black ash geopolymerization.

4. Conclusions

The results of our study show that fresh black ash samples hydrated with plain water follow a steady growth trend in compressive strength development during the curing period of 90 days, with uniaxial compressive strength values reaching 8 MPa after 90 days of curing. XRD mineralogical analysis and SEM imagery show that the strength development in water-hydrated samples may be related to the formation of secondary Ca-Al-sulphate (ettringite, monosulphate) and hydrocalumite phases.

Ettringite/monosulphate forms needle-like structures that fill the pore space and interlock with each other to form a structural matrix. Samples activated with NaOH solution show comparable evolution but significantly lower compressive strength values. We suggest that the reason for the lower strength achieved is the absence of the ettringite/monosulphate phase in NaOH-activated samples. Hydrocalumite precipitated instead of ettringite forms platy crystals that do not provide the interlocking structure as found in the ettringite-dominated water mixtures. We observed a clear peak in compressive strength in the NaOH-activated mixtures after 90 days of curing, which could be interpreted as being due to the formation of an amorphous geopolymer phase indicated by the increase in the amorphous phase content detected by the XRD analysis.

Na-silicate and Na-silicate/NaOH-activated samples show a strong geopolymerization and increase of Ca-Na-Al-silicate gel formation in the pore space of the ash aggregate. As a result, both mixtures already show high initial compressive strength values after 7 days of curing, amounting to 10.4 MPa in the sodium silicate-activated ash and to 7.75 MPa in Na-silicate/NaOH-activated samples. However, after 7 days, the microstructure of these gels already shows development of dense crack systems that penetrate the samples, resulting in a remarkable drop in compressive strength after 28 and 90 days of curing. The reason for microdeformation development could lie in the significant dry-shrinkage of the geopolymer pastes. For geopolymeric binder production using oil shale SHC ash, further research on the causes and prevention of Ca-Na-Al-silicate gel shrinkage is needed.

REFERENCES

1. Provis, J. L., Bernal, S. A. Geopolymers and related alkali-activated materials. *Annu Rev Mater Res*, 2014, **44**, 299–327.
2. Ots, A. *Oil Shale Fuel Combustion*. Tallinna Raamatutrükikoda, Tallinn, 2006.
3. Kearns, J., Tuohy, E. Trends in Estonian oil shale utilization: October 2015. *Analysis: International Centre for Defence and Security* (Tuohy, E., ed.). International Centre for Defence and Security, Tallinn, 2015. Available at http://www.digar.ee/id/nlib-digar:268094
4. Liive, S. Oil shale energetics in Estonia. *Oil Shale*, 2007, **24**(1), 1–4.
5. Mõtlep, R., Kirsimäe, K., Talviste, P., Puura, E., Jürgenson, J. Mineral composition of Estonian oil shale semi-coke sediments. *Oil Shale*, 2007, **24**(3), 405–422.
6. Siirde, A., Eldermann, M., Rohumaa, P., Gusca, J. Analysis of greenhouse gas emissions from Estonian oil shale based energy production processes. Life cycle energy analysis perspective. *Oil Shale*, 2013, **30**(2S), 268–282.
7. Bauert, H., Kattai, V. Kukersite oil shale. In: *Geology and Mineral Resources of Estonia* (Raukas, A., Teedumäe, A., eds.). Estonian Academy Publishers, Tallinn, 1997, 313–327.
8. Mõtlep, R., Sild, T., Puura, E., Kirsimäe, K. Composition, diagenetic transformation and alkalinity potential of oil shale ash sediments. *J. Hazard. Mater.*, 2010, **184**(1–3), 567–573.
9. Reinik, J., Heinmaa, I., Mikkola, J.-P., Kirso, U. Hydrothermal alkaline treatment of oil shale ash for synthesis of tobermorites. *Fuel*, 2007, **86**(5–6), 669–676.
10. Reinik, J., Heinmaa, I., Kirso, U., Kallaste, T., Ritamäki, J., Boström, D., Pongrácz, E., Huuhtanen, M., Larsson, W., Keiski, R., Kordás, K., Mikkola, J.-P. Alkaline modified oil shale fly ash: Optimal synthesis conditions and preliminary tests on CO_2 adsorption. *J. Hazard. Mater.*, 2011, **196**, 180–186.
11. Richardson, I. G. Tobermorite/jennite- and tobermorite/calcium hydroxide-based models for the structure of C-S-H: applicability to hardened pastes of tricalcium silicate, beta-dicalcium silicate, Portland cement, and blends of Portland cement with blast-fumace slag, metakaolin, or silica fume. *Cement Concrete Res.*, 2004, **34**(9), 1733–1777.
12. Golubev, N. Solid oil shale heat carrier technology for oil shale retorting. *Oil Shale*, 2003, **20**(3), 324–332.
13. Talviste, P., Sedman, A., Mõtlep, R., Kirsimäe, K. Self-cementing properties of oil shale solid heat carrier retorting residue. *Waste Manage. Res.*, 2013, **31**(6), 641–647.
14. Mindess, S., Young, J. F., Darwin, D. *Concrete*. Second Edition. Prentice Hall, Pearson Education, Inc., Upper Saddle River, NJ, 2003.
15. Sedman, A., Talviste, P., Kirsimäe, K. The study of hydration and carbonation reactions and corresponding changes in the physical properties of co-deposited oil shale ash and semicoke wastes in a small-scale field experiment. *Oil Shale*, 2012, **29**(3), 279–294.
16. Sedman, A., Talviste, P., Mõtlep, R., Jõeleht, A., Kirsimäe, K. Geotechnical characterization of Estonian oil shale semi-coke deposits with prime emphasis on their shear strength. *Eng. Geol.*, 2012, **131–132**, 37–44.

17. Kuusik, R., Uibu, M., Kirsimäe, K., Mõtlep, R., Meriste, T. Open-air deposition of Estonian oil shale ash: formation, state of art, problems and prospects for the abatement of environmental impact. *Oil Shale*, 2012, **29**(4), 376–403.

18. Baur, I., Keller, P., Mavrocordatos, D., Wehrli, B., Johnson, C. A. Dissolution-precipitation behaviour of ettringite, monosulfate, and calcium silicate hydrate. *Cement Concrete Res.*, 2004, **34**(2), 341–348.

19. Liira, M., Kirsimäe, K., Kuusik, R., Mõtlep, R. Transformation of calcareous oil-shale circulating fluidized-bed combustion boiler ashes under wet conditions. *Fuel*, 2009, **88**(4), 712–718.

20. Clark, B. A., Brown, P. W. Formation of ettringite from monosubstituted calcium sulfoaluminate hydrate and gypsum. *J. Am. Ceram. Soc.*, 1999, **82**(10), 2900–2905.

21. Gilbert, I. Creep and shrinkage models for high strength concrete – Proposals for inclusion in AS3600. *Aust. J. Struct. Eng.*, 2002, **4**(2), 95–106.

22. Castel, A., Foster, S. J., Ng, T., Sanjayan, J. G., Gilbert, R. I. Creep and drying shrinkage of a blended slag and low calcium fly ash geopolymer Concrete. *Mater. Struct.*, 2016, **68**(5), 1619–1628.

23. Bažant, Z. P. Prediction of concrete creep and shrinkage: past, present and future. *Nuc. Eng. Des.*, 2001, **203**(1), 27–38.

24. Ridtirud, C., Chindaprasirt, P., Pimraksa, K. Factors affecting the shrinkage of fly ash geopolymers. *Int. J. Min. Met. Mater.*, 2011, **18**(1), 100–104.